Received: 13 April 2020 | Revised: 17 April 2021 | Accepted: 22 April 2021

DOI: 10.1002/navi.424

ORIGINAL ARTICLE

WILEY ION

Automatic Dependent Surveillance-Broadcast (ADS-B) Universal Access Transceiver (UAT) transmissions for Alternative Positioning, Navigation, and Timing (APNT): Concept & practice

Sherman Lo | **Yu-Hsuan Chen**

Stanford GPS Lab, Aeronautics & Astronautics Department, Stanford University, California, USA

Correspondence
Dr. Sherman Lo, Stanford GPS Lab, Aeronautics & Astronautics Department, Durand Hall, Room #250, 496 Lomita Mall, Stanford, CA 94305-4035
Email: daedalus@stanford.edu

Funding information
Federal Aviation Administration, Grant/Award Numbers: 2008-G-07-3, 693KA8-19-N-00015

Abstract

The vulnerability of Positioning, Navigation, and Timing (PNT) services derived from Global Navigation Satellite Systems (GNSS) makes having a resilient and accurate Alternative PNT (APNT) based on high-power terrestrial radio sources necessary. The L-band is very crowded spectral real estate with GNSS, Distance Measuring Equipment (DME) and Air Traffic Control Beacon System (ATCRBS) signals occupying the band from 900–1600 MHz. Thus, as getting new signal and spectrum for APNT would be difficult, we must leverage existing transmissions and infrastructure. The ~660 Automatic Dependent Surveillance-Broadcast (ADS-B) ground stations in the United States represent significant infrastructure that can be leveraged for APNT. However, as ADS-B was designed for surveillance, it does not inherently possess features necessary to support APNT goals. This paper describes and demonstrates techniques for using ADS-B Universal Access Transceiver (UAT) signals for PNT. We develop methods to use all ground UAT signals to provide robust, multi-frequency pseudoranges. We examine the ranging and positioning performance of the UAT signal on the ground and in flight, to demonstrate its ranging accuracy, and hence the timing and synchronization of the station. We demonstrate and analyze navigation using UAT signals, as well as the intra-system interference challenges of using multiple UAT stations.

KEYWORDS
APNT, ADS-B UAT

1 | INTRODUCTION

Alternative or Complimentary Positioning, Navigation, and Timing (APNT/CPNT) systems can play a vital role in the robustness of Position, Navigation, and Timing (PNT) infrastructure. We have become so reliant on the PNT services provided by GNSS that it is considered critical safety infrastructure. GNSS-derived services are vital for numerous critical infrastructure applications, from power grid synchronization to telecommunications to financial transactions, to all forms of transportation – in the air, on the water, and on the ground. As GNSS has proliferated, so have the threats to its use to support critical operations. GNSS interference, both jamming and spoofing - and

especially intentional interference - is becoming more and more common. Furthermore, GNSS spoofing is becoming more accessible and affordable.

Given the likelihood of these threats, the US Federal Aviation Administration (FAA) has developed and examined several candidate solutions to provide APNT. Starting around the year 2000, the FAA developed an enhanced long-range navigation (eLORAN) to serve as APNT. While eLORAN had potential to serve as a multimodal APNT (Federal Aviation Administration, 2004), the system was not owned or managed by the FAA, and its infrastructure was shut down in 2010. The FAA APNT program, which started around 2009, examined using FAA-managed systems to address GNSS reliance in aviation (Eldredge et al., 2010). These included systems for navigation such as Distance Measuring Equipment (DME), Very High Frequency (VHF) Omni-Directional Ranging (VOR), and Non-Directional Beacons (NDB); surveillance such as Automatic Dependent Surveillance Broadcast (ADS-B); and data such as Automated Weather Observing System (AWOS). The APNT team developed several possibilities for improving existing FAA terrestrial radio systems to provide data and passive ranging suitable for providing operational compliments to GPS/GNSS, particularly to support future airspace and Next Generation Air Transportation System (NextGen) navigation and surveillance operations. In the end, three major options were studied in detail – DME, pseudoranging (using DME, ADS-B, and other aviation signals) and multi-lateration, where synchronized ground stations gather ranges from aircraft transmissions to determine the aircraft's position (Lilley & Erikson, 2012; Lo, 2012; Lo, Enge et al., 2015; Niles, et al., 2012).

There are many reasons for developing ranging and time signals using aviation systems such as ADS-B Universal Access Transceiver (UAT). The infrastructure already exists and APNT capabilities may be gained without affecting current systems and operations. Even if other potential APNT systems are available, such as enhanced DME, having UAT ranging and time is very valuable to provide additional signals. ADS-B and DME stations are not collocated, and combining the roughly 660 ADS-B (Federal Aviation Administration, 2018) with the about 1,100 DME stations in the United States significantly increases the signals available over DME alone. This is important, because these APNT systems are terrestrial and transmit in line-of-sight (LOS) bands such as the L-band. With stations near the ground and signals that propagate LOS, they cannot be received at low altitude farther away from the station due to the radio horizon of the transmission. Low altitude is where APNT is most needed, as the most critical part of a flight, approach and landing, occurs here. By combining DME and ADS-B ranges, we get signals from more transmitter locations, which helps improve low-altitude coverage. Finally, even though the FAA's APNT efforts have been superseded by other GNSS resiliency efforts, there is continued interest around the world in APNT (Jheng, et al., 2020; Kim & Kee, 2019; Schneckenburger, et al., 2018). The concepts that were developed are useful to support other airspace needs, such as providing robust time and helping to comply with federal policy to ensure the resiliency of PNT services (Executive Office of the President, 2020; White House Administrative Office, 2004). The Department of Transportation (DOT) and FAA are currently (2020) examining the use of some APNT concepts, such as enhanced DME and ADS-B UAT to provide robust sources of precise time (Lo & Chen, 2020).

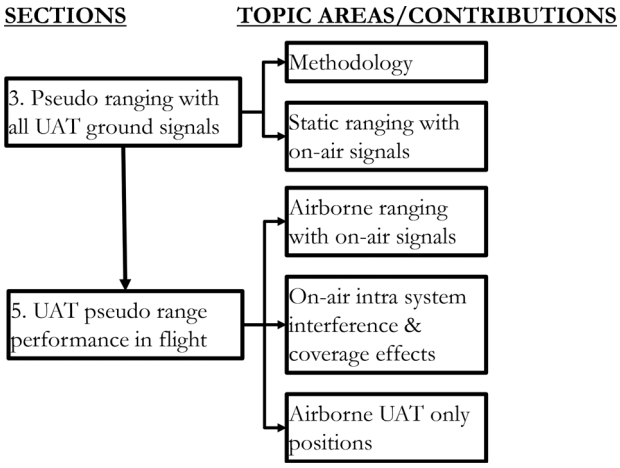

FIGURE 1 Major sections and contributions of the paper

1.1 | Outline

This paper covers methods of employing ADS-B UAT signals for navigation and timing, as well as its performance and challenges. First, the paper provides background on ADS-B UAT and the potential benefits of its use for aviation navigation. The main body of the paper is outlined in Figure 1. In Section 3, we develop methods for using the ADS-B UAT signals for ranging and timing. A method is developed that allows for use of ground transmissions that do not have inherent pseudoranging capabilities. This method is demonstrated using ground measurements. As a result, we show that nearly all ground transmissions may be used for ranging without change to the message content. Sections 4 and 5 describe UAT flight tests and show the performance of UAT pseudoranging in these tests, respectively. These tests allow us to receive UAT signals from multiple stations and examine the benefits and challenges of using these signals for aviation navigation. Key findings focus on ranging accuracy in flight, intra-system interference and analysis and display of its coverage effects, and

TABLE 1 Comparison of Mode S ES and UAT for ADS-B

Protocol	Advantages	Disadvantages
Mode S ES	International standard Widely adopted	Requires changes to signal to provide ranging Frequency congestion (used by other aviation systems)
UAT	Provides PNT with minimal changes Higher data rates, more message data capacity Dedicated frequency	US standard, not as commonly used Intra-system interference

demonstrating the UAT-only positioning. Hence, three key areas of UAT-based APNT are covered in this paper: how to do ranging with UAT, range/positioning performance, and the effects of interference on availability/coverage.

2 | ADS-B UAT BACKGROUND

While the worldwide deployment of ADS-B has created another dependency on GNSS, it has also created significant ground-based infrastructure, under the control of Air Navigation Service Providers (ANSPs), that may be useful for mitigating the impacts of GNSS interference. Two protocols exist for ADS-B in the United States: Mode Select (Mode S) Extended Squitter (ES) on 1090 MHz - which has been adopted worldwide - and UAT on 978 MHz. Mode S ES is compatible with legacy transponder equipment and protocols. Hence, it is attractive to air carriers that already carry Mode S transponders. UAT is attractive for APNT in the United States, as it represents a newer design without need for the legacy compatibility and interoperability that limits Mode S ES. Compared to Mode S ES, UAT has higher data rates, more efficient bandwidth usage, and requires only minor additions to provide accurate pseudoranges. Table 1 shows a simple comparison of these two ADS-B protocols.

To understand the potential utility of ADS-B UAT for navigation and timing, we provide some background on its deployed infrastructure, the use of this infrastructure for aviation navigation and timing, and the UAT transmissions, including its message structure and transmission segments.

2.1 | Automatic Dependent Surveillance - Broadcast (ADS-B) infrastructure

The ADS-B system in the United States, including the Gulf of Mexico, is enabled by the deployment of approximately

FIGURE 2 ADS-B radio stations deployed in the conterminous United States (CONUS) [Color figure can be viewed in the online issue, which is available at wileyonlinelibrary.com and www.ion.org]

660 ADS-B ground stations, known as radio stations (RS) (Federal Aviation Administration, 2018). This is shown in Figure 2. The stations receive ADS-B spontaneous transmissions ("squits") from aircraft that provide aircraft position and other data. They provide surveillance, situational awareness and other information from the ANSPs to local aircraft. The US RSs transmit on both Mode S ES and UAT protocols (Federal Aviation Administration, 2018). Both protocols provide aircraft Secondary Surveillance Radar (SSR) information through their Traffic Information Service Broadcast (TIS-B) and rebroadcast of ADS-B reports, known as Automatic Dependent Surveillance Rebroadcast (ADS-R), in which airborne messages transmitted on one protocol are re-sent by the ground using the other protocol. UAT also provides weather information through its Flight Information Services Broadcast (FIS-B). These additions offer valuable services to its targeted users - general aviation - who often do not have Mode S transponders. This is shown in Figure 3.

These ADS-B RS are commonly installed on commercial cellular (as shown in Figure 4) or dedicated towers. An ADS-B RS typically uses one omnidirectional UAT antenna and four directional Mode S ES antennas. The Mode S ES antenna has a 90-degree, 3 decibel (dB) beam width on the azimuthal plane.

2.2 | ADS-B for navigation and timing

While ADS-B was designed and deployed to support the Air Traffic Control (ATC) surveillance functionality, ADS-B infrastructure can provide accuracy, continuity, integrity, and coverage benefits for navigation and timing. Like other APNT possibilities being studied for aviation, such as DME and L-Band Digital Aviation Communications (L-DACS) (Schneckenburger et al., 2013, 2018), it operates at around

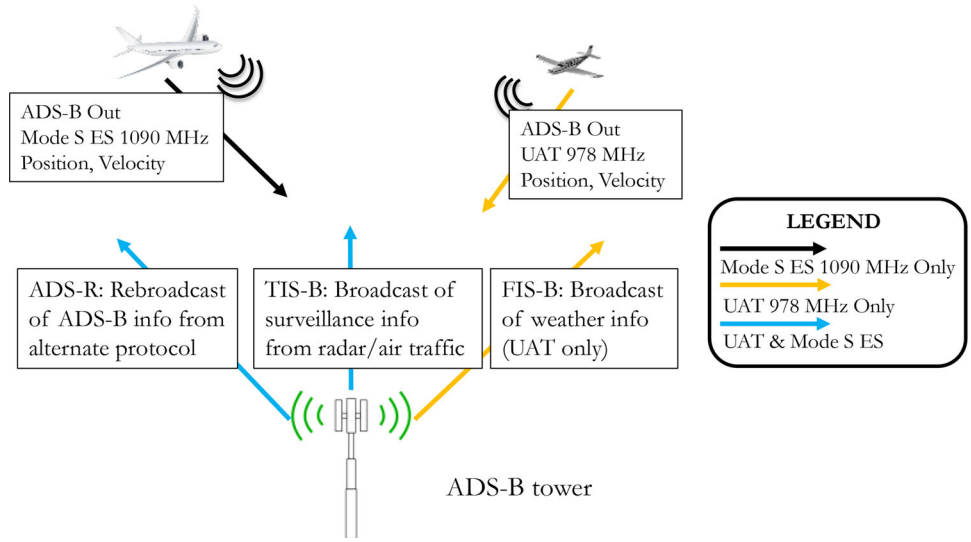

FIGURE 3 Transmissions from ADS-B radio stations and ADS-B-equipped aircraft [Color figure can be viewed in the online issue, which is available at wileyonlinelibrary.com and www.ion.org]

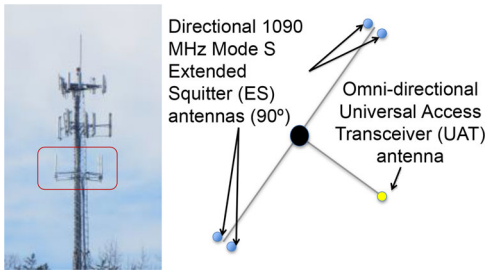

FIGURE 4 Leon, West Virginia, ADS-B radio station on cellular tower (L) and notional antenna layout (R) [Color figure can be viewed in the online issue, which is available at wileyonlinelibrary.com and www.ion.org]

FIGURE 5 DMEs (squares), Tactical Air Navigation (TACANs) (circles), and ADS-B radio stations (pins) deployed in CONUS [Color figure can be viewed in the online issue, which is available at wileyonlinelibrary.com and www.ion.org]

1000 MHz and in an Aeronautical Radio Navigation Service (ARNS) band that is protected for aviation use. A benefit of using ADS-B is to help support navigation in airport terminal areas, where aircraft are closer to the ground and fewer terrestrial stations are available due to LOS limitations. Our previous analysis has shown that using the roughly 660 ADS-B RS used with the 1,100 DME stations in CONUS can provide significant coverage improvements over DME alone for NextGen terminal area operations (Lo et al., 2011, 2014). Figure 5 shows a map of ADS-B RS and DME stations in CONUS. Even greater improvements can be achieved when these signals can be combined using the hybrid APNT concept (Lo et al., 2014), which combines pseudoranges with true ranges. Of course, a necessary condition for such capabilities using ADS-B is accurate knowledge of Time of Transmission (TOT), which enables pseudoranging and time synchronization. Next, we discuss the UAT transmission to understand when and how we can derive its TOT.

2.3 | UAT transmissions

The key to understanding UAT for navigation is to understand its channel design. The UAT channel is organized into one-second-long frames, ideally starting at each UTC second. This frame is divided into two segments: Ground and ADS-B. Transmissions are only allowed at specific times relative to the UTC second, known as Message Start Opportunities (MSO). MSOs are uniformly spaced and 250 microseconds (μs) apart, starting and ending 6 milliseconds (ms) after and before the UTC, respectively. These 6 ms periods before and after the UTC second provide guard bands between the segments. There is a 12 ms guard band that begins 182 ms after a UTC second that separates the end of the Ground Segment and the beginning

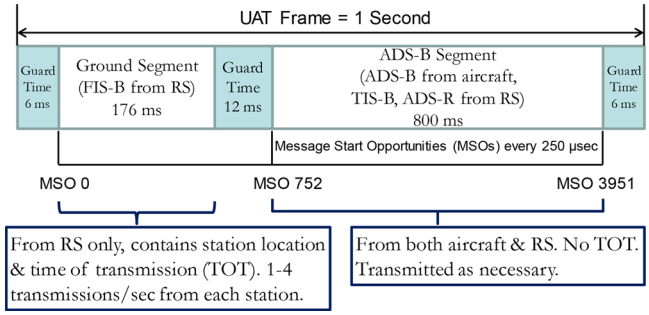

FIGURE 6 UAT frame and transmission structure based on descriptions and diagrams from (RTCA Special Committee-186, 2009) [Color figure can be viewed in the online issue, which is available at wileyonlinelibrary.com and www.ion.org]

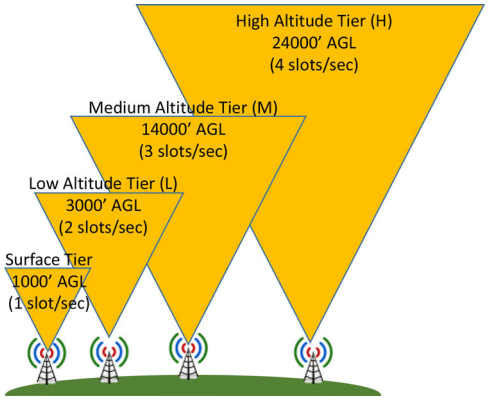

FIGURE 7 UAT ADS-B radio station tiers based on (Federal Aviation Administration Surveillance and Broadcast Services (SBS) Program Office, 2013) [Color figure can be viewed in the online issue, which is available at wileyonlinelibrary.com and www.ion.org]

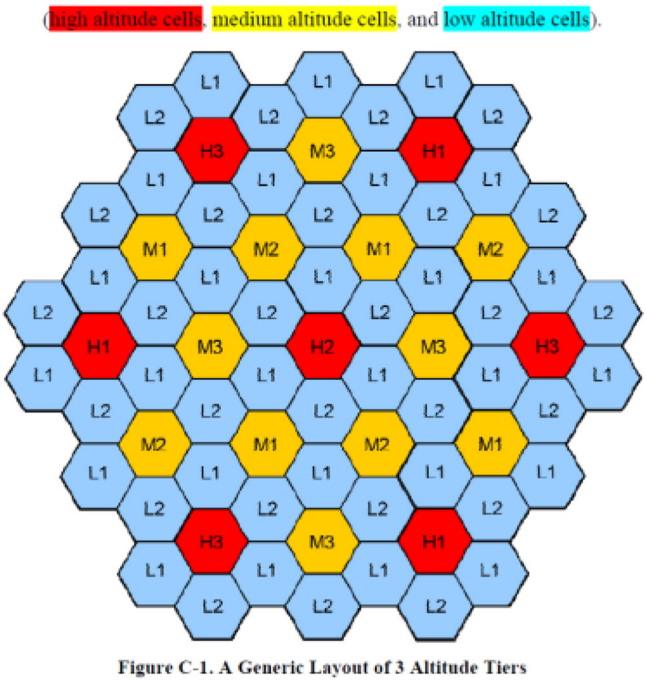

FIGURE 8 Notational layout of station tiers (L = low, M = medium, H = high, number = slot set used) figure from (Federal Aviation Administration Surveillance and Broadcast Services (SBS) Program Office, 2013) [Color figure can be viewed in the online issue, which is available at wileyonlinelibrary.com and www.ion.org]

of the ADS-B Segment. The Time Division Multiple Access (TDMA) structure of UAT is shown in Figure 6.

The UAT signal is modulated through Continuous Phase Frequency Shift Keying (CPFSK) with the signal frequency varying by ±312.5 kHz. CPFSK keeps the transmitted energy mainly within a 1 MHz DME channel. An increase of 312.5 kHz (Δf) indicates a "1" bit, while the same decrease indicates a "0" bit. Each UAT transmission uses a synchronization header consisting of 36 0.96 μs long bits. While the bit period is roughly the same as that for Mode S ES, the UAT message structure and organized channel (slotted ALOHA) allow for longer messages, larger payload, and higher data rates compared to the pure ALOHA random transmissions for Mode S ES (Federal Aviation Administration Surveillance and Broadcast Services (SBS) Program Office, 2013). The synchronization bit sequence used for the ADS-B segment are the inverse of those used in the ground segment.

In the ground segment, only transmissions (i.e. FIS-B) from ground stations are allowed. Transmissions are further limited to being started at only 32 uplink opportunities or slots for each second, with adjacent slots separated by 5.5 ms (i.e. 22 MSOs apart). A ground station regularly transmits in one to four of the allowed 32 slots in each given second. The number depends on its service altitude with one, two, three, and four messages transmitted in these slots per second for the surface-, low-, medium- and high-altitude tier stations, respectively. This is shown in Figure 7. Each service tier has designated sets of transmission slots that are used exclusively by that tier at any given second. So, a station at one service tier will not use a slot currently designated for a station at a different service tier. We will show later that a message transmitted in one slot should not interfere with messages transmitted in other slots, including adjacent ones. The consequence of the above statements is that only stations in the same tier using the same slot set may interfere with each other. Hence, stations serving different tiers will not interfere with each other, as they do not transmit in the same slots. The stations are organized using a cellular layout with multiple low-, fewer medium-, and even fewer high-altitude stations serving each region. This is notionally shown in Figure 8.

The system is designed such that a user can always receive the FIS-B messages needed for the airspace it is in.

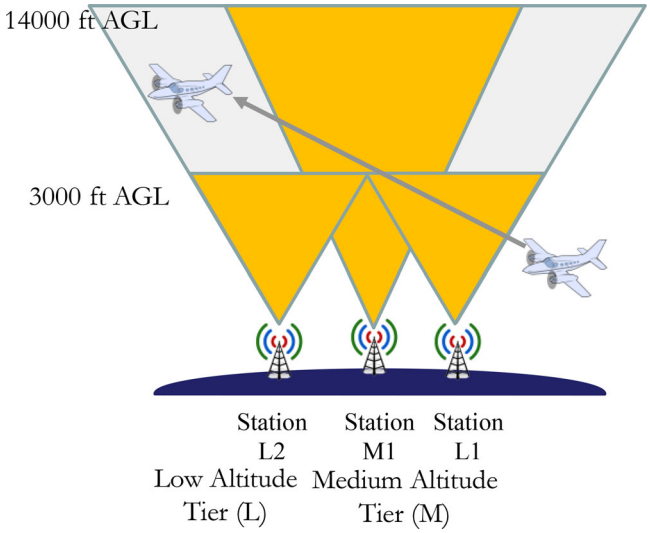

FIGURE 9 Example of UAT coverage from low-to-medium altitude tier; L and M tier station targets providing coverage to aircraft below 3,000 and 14,000 ft above ground level (AGL), respectively. Above 3,000 ft AGL, L tier stations may interfere with each other [Color figure can be viewed in the online issue, which is available at wileyonlinelibrary.com and www.ion.org]

Figure 9 illustrates the concept. An aircraft starts at low altitude and can receive low-altitude tier station L1. While station L2 may interfere as it uses the same slots, this will only happen when the aircraft is at an altitude high enough where the station L2 is within the radio horizon of the aircraft. By this point, the aircraft is at a higher altitude and would have a medium-altitude tier station (M1) available for data. The medium-altitude station transmissions will not be interfered with by the low-altitude stations. They will contain all the data from receivable low-altitude stations, plus additional information to cover the larger coverage area of the medium-altitude station - it has more transmission slots than low-altitude stations. The design guarantees data availability but reduces available signals for ranging as it essentially has built-in intra-system interference – something we discovered in our flight tests.

Each ground segment FIS-B message contains 4,416 bits plus a 36-bit synchronization sequence. The actual message data payload is 3,456 bits (432 bytes), which includes an 8-byte header. The reduction is due to application of forward error correction (FEC). Since each bit takes 0.96 μs, ground segment messages are about 4.274 ms long. Since adjacent slots are separated by 5.5 ms, a message from one slot is unlikely to interfere with that transmitted in another. The 1.23 ms difference between the message length and slot interval represents about 368 kilometers (km) of distance for an electromagnetic (EM) signal. For two transmissions from adjacent slots to interfere, the earlier transmission would have to be from at least 368 km further away. This distance is beyond the design range of UAT transmissions.

The ADS-B segment contains ADS-B transmissions from aircraft as well as ADS-R and TIS-B from RSs. In this segment, every MSO may be used for a transmission. Hence, there are more possibilities for interference. ADS-B segment messages are much shorter and contain less data than the ground segment messages. Two message form factors are defined: 1) basic message that is 272 bits (264.96 μs) long and 144 bits of data payload, and 2) long message that is 420 bits (403.2 μs) long that provides 272 bits of data payload. The additional bits in those messages are used to support FEC and synchronization. Transmissions from adjacent MSOs could easily interfere. However, it is attractive to use ADS-B segment for navigation and time because it can provide many more transmissions than the ground segment and it occupies much of each 1 second UAT epoch.

The next section will discuss pseudoranging using UAT ground transmissions. The ground segment messages (FIS-B) contain the basic information (TOT, station location) needed for pseudoranging, whereas ADS-B segment messages do not contain this information. Hence, the ADS-B segment messages cannot be directly used for pseudoranging without aid or modification. The focus of the next section addresses this issue.

3 | PSEUDORANGING WITH UAT

This section develops and demonstrates how ground transmissions (TIS-B, ADS-R) from the ADS-B segment also can be used for pseudoranging by leveraging information from prior messages. The developed technique allows nearly all ground transmissions to be used for basic ranging without change to the message content. Some changes may be needed to support higher accuracy and integrity. The final part of the section uses static ground measurements to assess the methodology and the performance of ranging using ADS-B segment ground message.

3.1 | Providing pseudoranging and timing with UAT overview

The regularly transmitted UAT FIS-B messages contain much of the required information for pseudorange in their message headers: station location in the form of latitude and longitude, as well as station identification, and TOT in the form of the slot ID (0 to 31). The slot ID can be converted to TOT (relative to the UTC second) by Equation 1. Hence, it practically contains everything needed for

pseudoranging in the ground segment transmission.

$$TOT = 6 + 5.5 \cdot (slot\ ID)\ ms \quad (1)$$

However, it is not fully sufficient for the highly reliable and accurate navigation, precise time transfer or absolute time. The UAT signal, as described in the current UAT Minimum Operational Performance Specifications (MOPS) (RTCA Special Committee-186, 2009), still has several limitations for time synchronization and navigation with integrity. Specifically: 1) It cannot indicate if the transmission timing variation is less than 500 nanoseconds (ns) off UTC; 2) it does not provide absolute time information (e.g., time of week in seconds, week number relative to a start week); and 3) it only allows for an approximately 1 Hz range update rate.

The first is of great import for trusted navigation and timing. A FIS-B message contains a coarse integrity flag for synchronization to UTC, indicating whether the transmission is or is not within 500 ns of UTC. As the message has significant data capacity, it also may be possible to use a few bits for additional integrity alerts related to ranging. One solution is to provide a fine synchronization flag that perhaps indicates different possible levels of time synchronization to UTC. Using only 2 bits, we could indicate the timing accuracy more precisely – for example: better than 250 ns, 100 ns, 50 ns or 10 ns time synchronization.

The second and third issues are relevant to time and navigation, respectively. A knowledge of which second the message is transmitted is needed to provide absolute time. This can be done in a similar way as GPS/GNSS with two fields – seconds since start of week (using 20 bits) and week number (using 11 bits, which would result in rollover every ~ 40 years). An ADS-B segment basic message is more than sufficient to provide this given the low data requirement. Additional unused capacity on a FIS-B message also could be used. On first glance, the 1 Hz update rate seems strange given there may be up to four ground segment transmissions per second for each ground station. However, these are all transmitted in the same 176 ms span each second, which means that we would go over 800 ms between two pseudorange measurements if using only ground segment messages from an RS, even if it transmitted multiple ground segment messages per second.

3.2 | Providing pseudoranging and timing with UAT

To achieve UAT pseudoranging measurements at a frequency much higher than 1 Hz requires that ADS-B segment transmissions from the ground (TIS-B, ADS-R) be used. The ADS-B segment messages in the current standards do not contain the necessary information for pseudoranging (RTCA Special Committee-186, 2009). Most importantly, the messages do not clearly provide TOT and identification of the ground station source. Other necessary information, such as station location and timing accuracy, may be gathered from the ground segment transmissions. One way of supplying TOT and source station identification could be achieved by developing and transmitting new ADS-B segment pseudoranging messages or extending existing messages. These methods would cost additional bandwidth and require changes to the MOPS and perhaps to the RSs. Therefore, we developed a way to use existing messages by creating a technique to determine the TOT and source identification from existing transmissions. In this way, we can use ADS-B segment message for pseudoranging without creating additional congestion to the spectrum and requiring modifications to existing infrastructure and transmissions.

We created a technique to determine TOT and source ground station identification by leveraging the information from the ground segment transmissions. From ground segment transmissions, we know the stations visible and the approximate corresponding pseudoranges. Over one UAT frame, the pseudorange from ground and ADS-B segment messages, denoted by PR_{GND} and PR_{ADSB}, respectively, should be close even for a fast-moving commercial aircraft - less than ~300 m. This is the distance traveled by an aircraft at 600 knots in one second. Since ground segment messages contain TOT, PR_{GND} is known, but we cannot immediately calculate PR_{ADSB} because there is no TOT information in the ADS-B segment messages. However, since TOT must occur at a specified MSO, we can generate an estimate of PR_{ADSB} for each received ADS-B segment message and use our known PR_{GND} to determine if the estimate is correct.

To make the estimate, we start with Equation 2, which shows that PR_{ADSB} equals the difference of time of arrival of the message at the aircraft (TOA_{AC}) from the TOT from the ground station (TOT_{GND}). Within a given second, the true TOT_{GND} equals the true transmission MSO (MSO_{true}) times 250 μs, since it must be transmitted at an MSO. For simplicity, the calculations shown neglect the initial 6 ms guard band offset from the UTC second seen in Figure 6. While we do not know MSO_{true}, we know that it differs from any other MSO (such as our initial estimate of the true MSO, MSO_{est}) by an integer multiple (N) of 250 μs – this is Equation 3 which we use to derive Equation 4. We can try different values of N and get corresponding guesses ($PR_{ADSB,est}$) for the pseudorange as per Equation 5. If we use the nearest MSO based on our time of arrival as our baseline guess, then the search space for N is

not large, as each unit change in N represents 75 km of distance and the transmission range of the ADS-B RS is less than 450 km. In this case, we only need to look at $N_{calc} = 0$ to 6 as possible values of N. The search space can be further reduced if we use received signal power to determine if the RS is close by or potentially far away.

From the various possible values of N_{calc} in Equation 5, we generate a set of possible pseudoranges. If the transmission comes from one of the stations, M, where we have a PR_{GND} for that UAT frame (i.e, second), then there should be a $PR_{ADSB,est}$ that is approximately equal to $PR_{GND,M}$ where $PR_{GND,M}$ is the ground segment pseudorange from station M calculated in that same UAT frame. If we can determine an N such that, for ground station M, $PR_{GND,M}$ and $PR_{ADSB,est}$ reasonably match, then we have determined the TOT (MSO_{est}+N) and identified the transmitting station (M). This is shown in Equation 6.

In fact, we do not even need to PR_{GND} if we have PR_{ADSB} from the prior second, as this pseudorange change over one second should be less than 300 m for even the fastest operational commercial aircraft, so PR_{ADSB} should differ from the current pseudorange by less than 300 m. Denoting the current time as n for each station, we can use either the current pseudorange from the ground segment, $PR_{GND,\ time\ n}$, or the prior second pseudorange from the ADS-B segment, $PR_{ADSB,time\ n-1}$, as our initial guess, $PR_{ADSB,init}$, and use it to calculate N (N_{calc}). While N_{calc} should be an integer, transmission time variations, measurement errors, and displacement between our prior measurement to current time will result in the calculation from Equation 8 to not be an integer. The main error is the aircraft displacement of about 300 m, or 1 μs over 1 second, clock drift, and measurement error. The latter two errors should be much smaller than the first. Thus, we may have about 1.5 μs of error due to aircraft displacement over 1.5 second. Additionally there may be a few tens of nanoseconds (ns) of other errors. This means that a correct N_{calc} should only differ from an integer value by 1.5 us/250 us or 0.006. This maximum deviation will be slightly increased by measurement noise but decreased for a slower aircraft. Note that the clock synchronization of the ground station does not matter with this method as we are essentially looking at a time difference, so absolute clock offsets are cancelled, leaving only clock drift. Theoretically, finding the correct N_{calc} allows us to get a pseudorange that is nearly as accurate as that derived from the ground segment transmissions.

$$\begin{aligned} PR_{ADSB} &= TOA_{AC} - TOT_{GND} \\ &= TOA_{AC} - MSO_{true} \cdot 250\ \mu s \end{aligned} \tag{2}$$

$$MSO_{true} = MSO_{est} + N \tag{3}$$

$$PR_{ADSB} = TOA_{AC} - (MSO_{est} + N) \cdot 250\ \mu s \tag{4}$$

$$PR_{ADSB,\ est} = TOA_{AC} - (MSO_{est} + N_{calc}) \cdot 250\ \mu s \tag{5}$$

$$\begin{aligned} PR_{ADSB,\ station\ M,\ time\ n} &\cong PR_{GND,\ station\ M,\ time\ n} \\ &= PR_{ADSB,\ init} \end{aligned} \tag{6}$$

$$PR_{ADSB,\ time\ n} \cong PR_{ADSB,\ time\ n-1} = PR_{ADSB,\ init} \tag{7}$$

$$N_{calc} = \frac{TOA_{AC} - PR_{ADSB,\ init}}{250\ \mu s} - MSO_{est} \tag{8}$$

An equivalent way to make the estimate is to calculate time of transmission assuming the signal is from one of the stations for which we have a ground segment pseudorange, $PR_{GND,}$ or an ADS-B segment pseudorange from a prior second. This is seen in Equation 9 for ground segment pseudoranges. If we can identify a station M with $PR_{GND,M}$ that results in a TOT close to a permitted transmission time or MSO (within ~ 300 m), then we have potentially identified the station and TOT.

$$TOT_{est,\ station\ M} = TOA_{AC} - PR_{GND,\ station\ M} \tag{9}$$

In rare instances, a user may have two or more different stations that satisfy the MSO criteria. We discuss three methods to handle this possibility in (Lo, Chen et al., 2015). One method is to use the ADS-B segment message itself. Some messages contain the six Least Significant Bits (LSB) of the transmit MSO, which could also be used to determine the source of ADS-B segment ground transmission and hence the correct TOT. Our measurements, which we used for our ranging analysis, show that this is not a commonly transmitted message. However, there are also spare bits, such as byte 18, from existing ADS-R/TIS-B messages that may be used to provide some information to resolve the ambiguity on the MSO and transmitting station. Finally, the MOPS indicate that the TIS-B message may contain four non-unique bits to help identify the transmitting station. The bits are not globally unique but potentially unique to stations in the vicinity.

3.3 | UAT pseudoranging demonstration

We conducted experiments to verify the technique using static data from two ADS-B ground stations near Stanford,

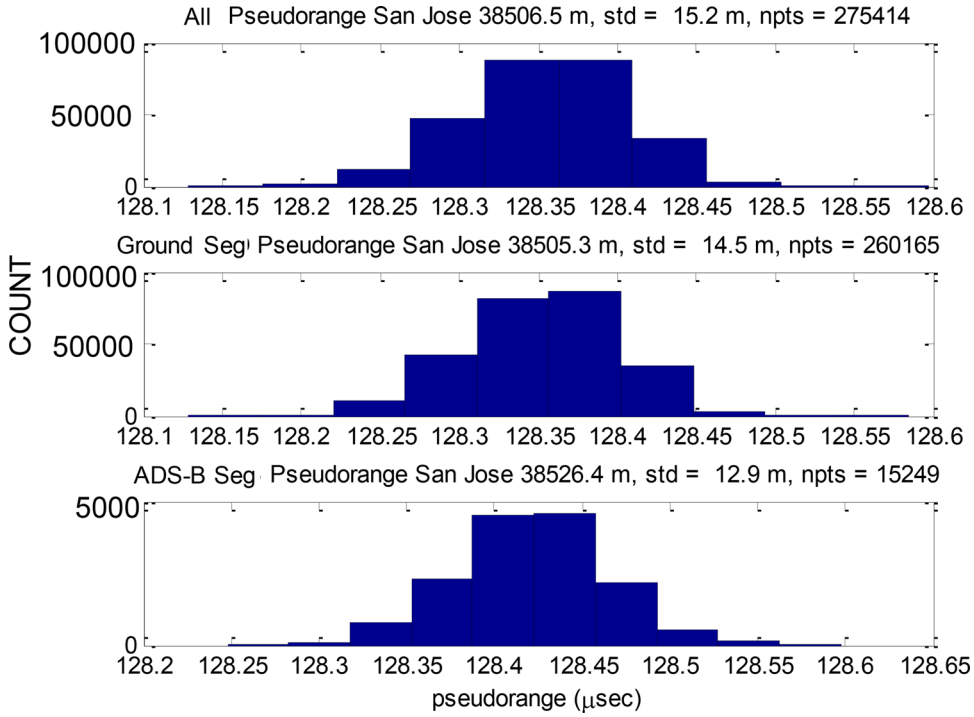

FIGURE 10 Histogram of pseudoranges from San Jose ADS-B radio station: All (top), Ground Segment (middle), ADS-B Segment (bottom) [Color figure can be viewed in the online issue, which is available at wileyonlinelibrary.com and www.ion.org]

California. The resulting pseudoranges from the ground segment and ADS-B segment match reasonably well. The process for calculating TOA with the software defined radio is described in (Chen et al., 2014). Figure 10 and Figure 11 show histograms of the ADS-B segment pseudoranges derived using the described technique (bottom) along with the ground segment pseudoranges (middle) and all pseudoranges (top) for the San Jose and Woodside ADS-B stations. The pseudoranges are close and imply that the MSOs are correctly estimated. But they also exhibit some differences with the mean of ADS-B segment pseudoranges exceeding that of the ground segment by about 15–20 m. This is common to measurements from both stations. The difference may be due to our simple processing, as the ground and ADS-B segments use different headers. This difference is not the result of error estimating the MSO, which would result in an error of at least 75 km (250 μs). For both segments and stations, the standard deviations of the pseudoranges are approximately 15 m.

4 | FLIGHT TEST OVERVIEW

Having developed and demonstrated the ability to generate pseudoranges from UAT transmissions, we then sought to demonstrate UAT-based navigation solutions. To support tests of ADS-B for navigation and tests of enhanced DME, Stanford University and Ohio University jointly conducted flight tests of APNT technologies in March 2015 (Lo, Chen et al., 2020). This flight test allowed for evaluation of key APNT technologies. UAT measurements were collected in the air and on the ground. As seen in Figure 12, elements on both the aircraft and the ground were fielded to support ADS-B testing.

The test aircraft used was a Beechcraft Baron fitted with a 19-inch avionics rack. This Ohio University aircraft test platform has been used on prior APNT testing (Li & Pelgrum, 2014). Onboard the test aircraft was an ADS-B experiment rack shelf, which contained data collection equipment for collecting raw signal samples of UAT and Mode S ES on 1090 MHz from a DME/ADS-B antenna on the underbelly of the aircraft. The signals coming in the antenna go through several signal protection components. One component was a limiter to suppress the effect of ownership transmissions. Another was a switch tied to the aircraft suppression bus which prevents our aircraft DME interrogations from entering into our data collection system. The signal was then split and sent to analog filters for UAT and 1090 MHz. Each signal had its own dedicated Universal Software Receiver Peripheral (USRP) using a daughter card to digitize the data, which was then sent to a data server where the raw radio frequency (RF) signals were stored for post processing by our software receiver. The USRPs were synchronized using the same 10 MHz clock input. This is shown in Figure 13. The Ohio University robust Inertial Measurement Unit (IMU) GPS

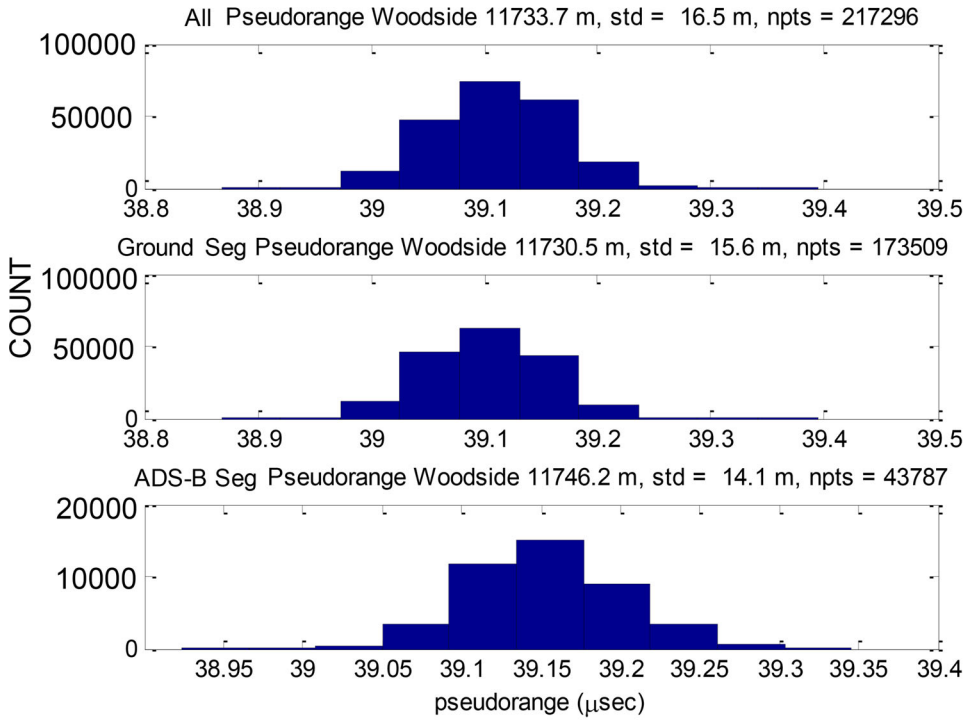

FIGURE 11 Histogram of pseudoranges from Woodside ADS-B radio station: All (top), Ground Segment (middle), ADS-B Segment (bottom) [Color figure can be viewed in the online issue, which is available at wileyonlinelibrary.com and www.ion.org]

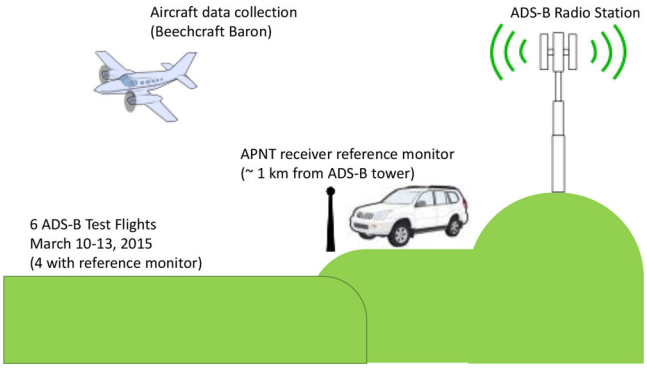

FIGURE 12 ADS-B elements of March 2015 flight test [Color figure can be viewed in the online issue, which is available at wileyonlinelibrary.com and www.ion.org]

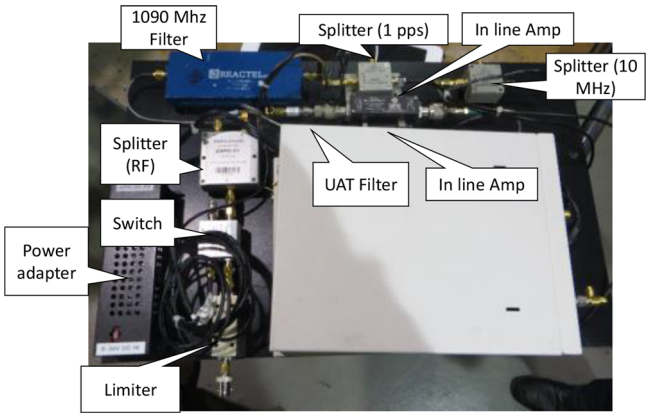

FIGURE 13 Airborne ADS-B collection rack shelf [Color figure can be viewed in the online issue, which is available at wileyonlinelibrary.com and www.ion.org]

Receiver (RIGR), which houses a Novatel OEM-V3 GPS, provided GPS observations and time tagging of the data and enabled precise time of arrival (TOA) determination. We further refined the time tag and GPS position data collected using a post-processed precise GPS service such as Canadian Spatial Reference System (CSRS) Precise Point Positioning (PPP).

Six test flights were performed from March 10–13, 2015. All six flights collected data suitable for assessing UAT performance. For four of the six flights, ground reference data were also collected. This paper will focus on UAT range, position, and interference.

Figure 14 shows a map with the composite ground track of the flights, along with the ADS-B radio stations observed. The flight tests were centered around Ohio University Airport. Two flights were check-out flights, while others were flown to gather data in a wheel-and-spoke pattern around the airport at different ranges and altitudes. The inner spoke and wheel were flown at ~3,300 feet above mean sea level (MSL) and the outer spoke and wheel were

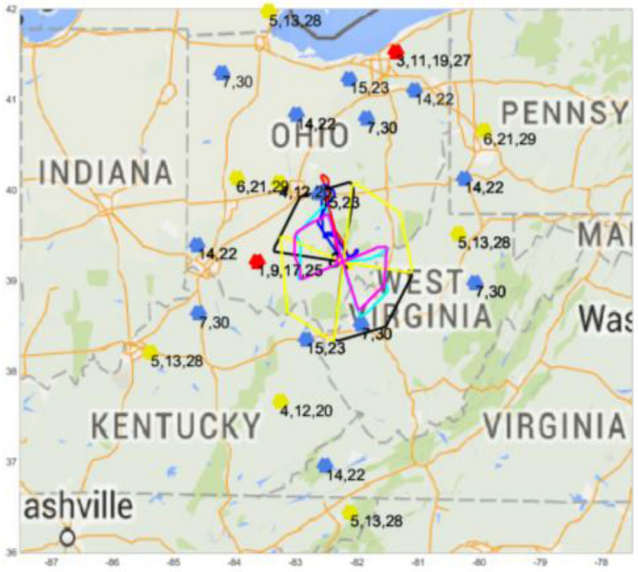

FIGURE 14 Test flight paths and ADS-B RS decoded (with slot numbers indicated) [Color figure can be viewed in the online issue, which is available at wileyonlinelibrary.com and www.ion.org]

TABLE 2 March 2015 flight altitudes

Date/Time	Cruise Altitude (MSL) ft
March 10 a.m.	6,000-7,000
March 10 p.m.	4,000-5,000
March 11 p.m.	10,500
March 12 a.m.	3,300
March 12 p.m.	10,300
March 13 a.m.	3,300

flown at ~10,000 feet MSL. The cruise altitude of each flight is shown in Table 2 where a.m. and p.m. indicate morning and afternoon flights, respectively. The airport is roughly at 650 feet MSL.

The flights decoded UAT broadcasts from stations Ohio (OH), Kentucky (KY), West Virginia (WV), Virginia (VA), Michigan (MI), Pennsylvania (PA) and Tennessee (TN). These stations are shown in the figure with low-, medium- and high-altitude ADS-B UAT RS denoted by blue, yellow and red markers, respectively.

5 | ANALYSIS OF UAT PERFORMANCE

The flight test data allows an examination of UAT performance not generally possible with ground testing. We assess range accuracy from multiple stations at a variety of ranges and altitudes. As multiple ranges are available, UAT position and position availability can be assessed. Finally, intra-system interference and its impact are assessed. This interference is only visible at altitudes where multiple distant stations can be received.

5.1 | Accuracy

Range accuracy is calculated by comparing the measured propagation time of the UAT FIS-B signal (i.e. ground segment messages) to the expected propagation time. Measured propagation time ($t_{prop,meas}$) is determined from the difference of measured TOA (TOA_{meas}) compared to the indicated TOT (TOT_{ind}) of the signal. Assuming that the ADS-B RS is synchronized to UTC, the measurement difference between the indicated TOT and measured TOA, as timed by UTC from GPS, is on the same time scale. Hence, we treat the time difference as a true time difference that yields a true range. The expected propagation time ($t_{prop,expected}$) is calculated using the range between the post-processed GPS position of the aircraft (xyz_{ac}) and the surveyed location of the ADS-B station (xyz_{adsb}). The expected propagation time also accounts for troposphere delay (Δ_{tropo}) using the Millman model (Millman, 1958) and assuming 100% humidity. This expected time represents the truth value, and the range error is the difference between measured and expected propagation times. The basic calculations are seen in Equations (10) and (11).

$$t_{prop,\,meas} = TOA_{meas} - TOT_{ind} \tag{10}$$

$$t_{prop,\,expect} = (\|xyz_{ac} - xyz_{adsb}\|_2)\ /c + \Delta_{tropo} \tag{11}$$

The resulting ranges should have errors introduced by processing, noise, multipath, equipment bias, GPS derived position, ADS-B station survey position and RS clock offset to the onboard GPS derived time. Some of the equipment bias can be eliminated by removing the average bias from all stations since this should be common mode. Figure 15 shows the range error after removing the average value over all stations as a bias. Even with this removal, the range error will still contain some bias, albeit much smaller and mostly due to clock error on each ADS-B RS. In the figure, there are outlier error points that are several standard deviations from the mean. The cause of the outliers is an integrity issue and merits further investigation. However, they are all within the 500 ns of UTC, and so are within synchronization tolerance allowed by the ADS-B RS for UAT.

From this data, the mean and accuracy (two standard deviations) of range error for each station on each flight is calculated. Figure 16 shows the location of the ADS-B

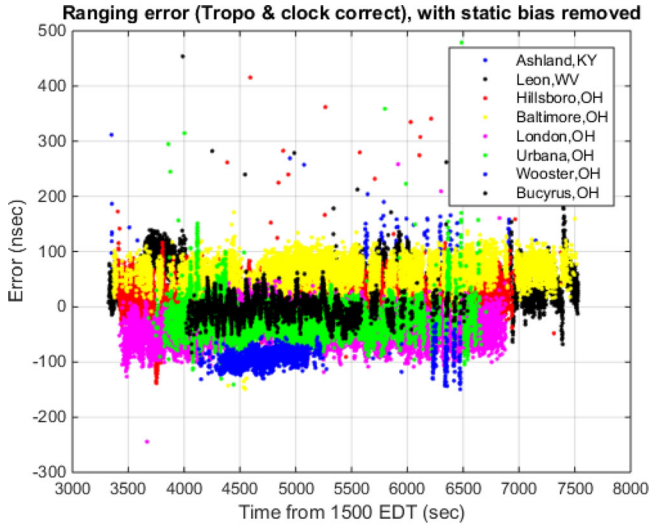

FIGURE 15 Range error from March 10, 2015, p.m. flight [Color figure can be viewed in the online issue, which is available at wileyonlinelibrary.com and www.ion.org]

RS seen in the analysis and their nominal ground segment transmission slots. Table 3 shows the mean, relative to the average bias over all stations, and the accuracies (two standard deviation or 2 σ) of the range error for the March 10 afternoon flight. This flight was at low altitude, and the stations visible were generally within about 120 km. The 2 σ accuracy is around 20 m. Table 4 shows the accuracy for all six flights. As suggested by the greater number of stations measured, the March 11 and 12 afternoon flights were conducted at a higher altitude over a longer distance. The range errors in these flights were slightly larger than the other. Stations on these flights can be received at larger ranges. Additionally, there was more intra system interference on these flights. Overall range accuracy typically measured between 20–30 m. However, this does not consider the bias errors which will exist partly because of ground station clock differences.

5.2 | Interference

The flight test also allowed us to examine the effects of intra-system interference due to transmission slot allocation. This interference was seen in the air, and Figure 17 shows an example of the interference between the signals from two UAT stations in the time domain. Without interference, ideally, a constant envelope signal with continuous phase changes should be seen. This interference was not seen on our ground measurements during the same time period.

Interference can potentially cause two issues: 1) loss of signal availability, and 2) increased range error. In this paper, we only explore the former, as the loss of signal can be clearly analyzed by comparing the number of received versus expected transmissions. The increased range error can be a more complex issue and is left for future analysis. The interference certainly can and does cause a multipath-like error. However, there are several ways to detect and mitigate this error. Detection can be done by decoding the messages and performing checks with the FEC and parity check. Detection and elimination of interfered signals may be suitable mitigation if there are many signals available. Our basic correlation processing did not attempt to remove the effect of the interference, but more advanced signal processing could mitigate the effect. A simple method is to use only the un-interfered portion of the signal which will be at the start of the message. This is fortuitous as it contains the most important components for ranging, such as the message header information and initial TOT. Also, it may be possible to know many of the transmitted bits from prior messages (such as the header), and a receiver may be able to process out some of the interfering signal.

In the flight test, signals were received from many stations, most of which were low-altitude tier stations. Figure 18 shows the flight paths, the stations received and their assigned slot numbers. Stations having the same slot numbers can interfere with each other. The blue, yellow, and red indicate low-, medium-, and high-altitude tier stations, respectively. For low-altitude stations, there are several stations that use the same set of slots, roughly four in the flight area shown. There are far fewer medium-altitude stations using common slots. The figure shows stations using the same slots circled with the same shade of blue or yellow. For the high-altitude stations, no stations with common slot numbers were in the vicinity.

5.3 | Interference effects on coverage

The effect of the interference on coverage is examined by looking at the range where message losses become significant. Figure 19 shows the average number of messages decoded as a function of distance for the March 10 afternoon flight. This flight was flown at 4,000-5,000 ft MSL. The figure shows the average for all low- and medium-altitude tier stations decoded, and the top line indicates how many seconds of data are available for the average. Recall that for low- and medium-altitude stations, receiving all messages means having two and three messages per second, respectively. On the plot for low-altitude tier stations (left side), there are three instances where the messages decoded drop off from the full reception value. The drop-off around 40–60 km is traced to aircraft maneuvers. At 80 km, transmission reception starts to drop off due

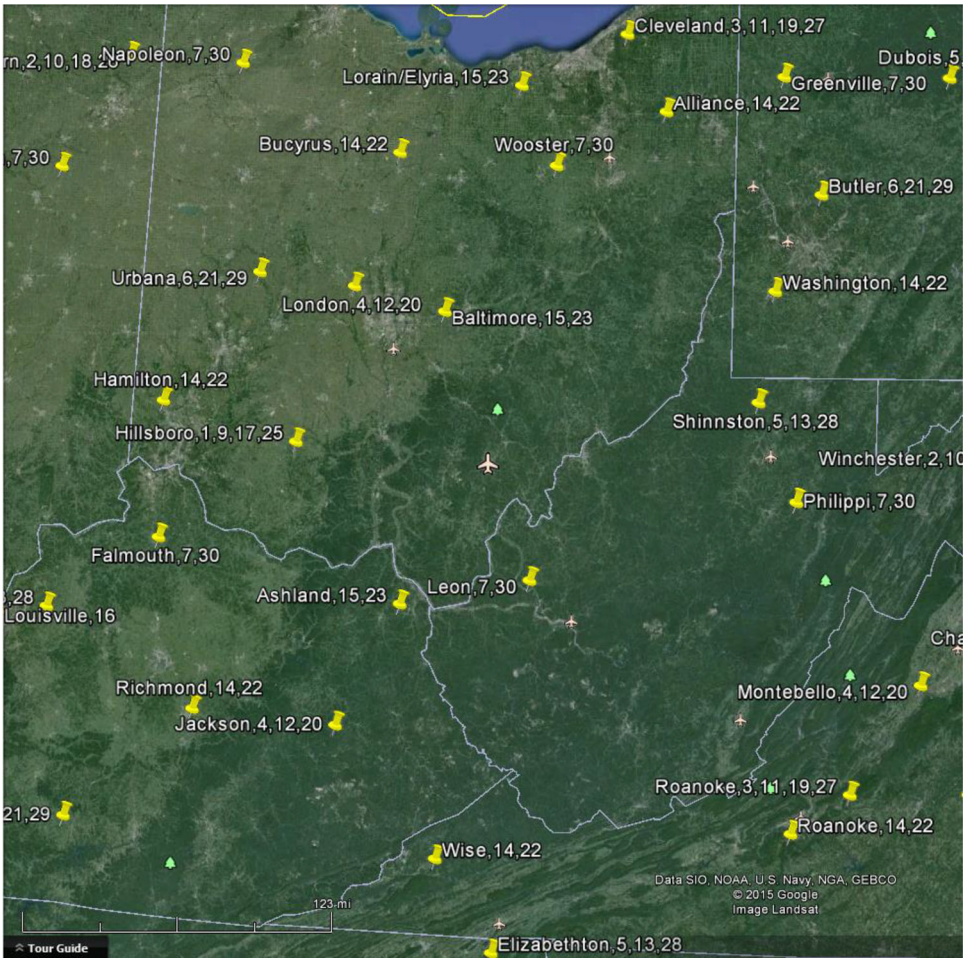

FIGURE 16 ADS-B radio stations in vicinity of flight test. Pin captions show station location name and UAT ground segment transmission slots assigned [Color figure can be viewed in the online issue, which is available at wileyonlinelibrary.com and www.ion.org]

TABLE 3 UAT range error on March 10 p.m. flight

Station	Mean (m)	Accuracy (m; 2 σ)
Ashland, KY	38.5	21.0
Leon, OH	10.4	24.9
Hillsboro, OH	3.2	19.6
Baltimore, OH	−3.2	26.1
London, OH	−19.7	16.9
Urbana, OH	−0.9	22.5
Wooster, OH	−28.9	15.4
Bucyrus, OH	1.5	16.2
Baltimore, OH (Ref)	-	12.6

potentially to intra-system interference. Near full reception returns at 100 km, but then reception again starts to decrease at a range of 120 km for other stations. For the plot with medium-altitude stations (right side), a sharp drop-off is seen around 150 km out. This is likely due to line-of-sight (i.e. radio horizon) limitation as the theoretical radio horizon at 4,000 ft MSL is about 160 km. Hence the significant message loss for medium-altitude stations only occurs due to radio coverage. This is expected as the design of the system is such that there should be little or no interference on the medium-altitude stations at our flight altitude.

Figure 20 shows a similar plot for the March 11 afternoon flight. This flight occurred at ~10,500 ft, where greater interference occurs for the low- and medium-altitude stations. For low-altitude stations, the average messages per second drops from its ideal value at 40 km and then more permanently at 80 km and beyond. This plot shows a higher level of interference than in the lower-altitude March 10 afternoon flight. For medium stations, the reception is near ideal up to a range of 80 km, has a slight drop to 2.5 messages up to a range of 120 km and then drops more afterwards. This shows more message loss and hence interference than seen in Figure 19. This is expected, as there should be more medium-altitude station interference since the aircraft is at a higher altitude.

TABLE 4 UAT range accuracy (m, 2σ), March 2015 flight tests

Station	3/10 a.m.	3/10 p.m.	3/11 p.m.	3/12 a.m.	3/12 p.m.	3/13 a.m.
Elizabethton, TN			26.7		24.0	
Wise, VA			23.2		16.7	
Jackson, KY			30.3		22.3	
Louisville, KY			18.0		18.5	
Ashland, KY		21.0	28.1	20.9	44.1	19.6
Leon, WV	17.6	24.9	26.4	27.5	18.6	25.4
Falmouth, KY					24.9	
Philippi, WV			22.6		15.6	
Hillsboro, OH	17.6	19.6	38.2	22.0	37.6	23.7
Hamilton, OH			32.5	18.8	31.3	22.0
Shinnston, WV	21.0		32.4	17.9	28.6	17.6
Baltimore, OH	27.5	26.1	29.7	23.2	19.0	23.6
London, OH	16.1	16.9	29.5	20.9	28.5	20.7
Washington, PA			20.0		20.0	19.8
Urbana, OH	17.7	22.5	29.3	32.8	30.6	19.2
Butler, PA			19.8		26.7	
Wooster, OH	18.4	15.4	23.2		15.4	
Bucyrus, OH	18.6	16.2	27.5	20.4	20.8	18.7
Cleveland, OH			26.8		22.5	

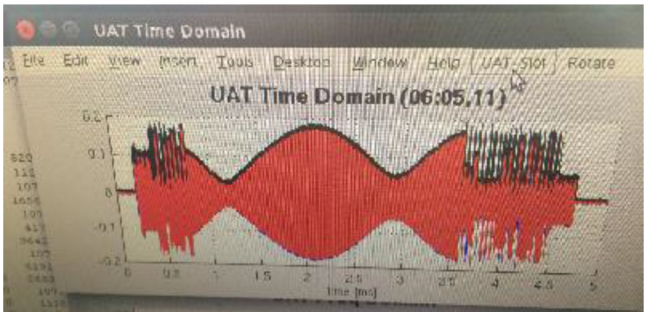

FIGURE 17 Interference between two UAT FIS-B on a signal amplitude (y-axis) versus time (x-axis) plot. Nominal UAT signal has constant amplitude envelope (Photo of inflight data display) [Color figure can be viewed in the online issue, which is available at wileyonlinelibrary.com and www.ion.org]

The coverage difference can be seen in Figure 21 and Figure 22, which show the reception of a low- (Baltimore, OH) and medium- (Urbana, OH) altitude station, respectively. The plots show where the aircraft received all, some (partial), or none of the signals from that station. The coverage area (providing full or partial reception) of the

FIGURE 18 Test flight paths and ADS-B RS decoded (with assigned slot numbers indicated); ADS-B RS sharing the same slots are circled with the same shade of color [Color figure can be viewed in the online issue, which is available at wileyonlinelibrary.com and www.ion.org]

medium-altitude station is significantly larger than that of the low-altitude station.

A key reason for using ADS-B for APNT is to have more ranging signals at low altitude. The radio horizon limits the reception of signals at range and, hence, may limit the impact of the most distant interference source(s) on coverage at low altitude. We calculate the relationship minimum altitude of the user versus the maximum distance, d, at which a signal is receivable. This distance, the radio horizon, was calculated using Equation 12 (radio horizon equation) with a standard k factor of 4/3 (4/3 earth radius model) (Haslett, 2008; Wikipedia). The k factor, which adjusts for the refraction of the radio signal in the atmosphere, can vary, but $k = 4/3$ generally models normal atmospheric conditions for line-of-sight RF signals (>30 MHz). The model is seen in Equation 12, where R is the radius of the earth and h_{tx} and h_{rx} are the transmitter antenna (ground station) and receiver antenna (aircraft) heights above earth. With $k = 4/3$, h_{tx} and h_{rx} in m, and d in km, the $\sqrt{2kR}$ term equals about 4.12.

Figure 23 shows the minimum altitude as a function of distance for which a signal from a transmitter on a 25 m tower is still in radio line of sight based on Equation 12. To illustrate, the figure shows that the value of the curve at a ground distance of 160 km is approximately 1,145 m. This means that an aircraft 160 km away from the transmitter would need to be at an altitude of at least 1,145 m (3,757 ft) to receive the transmitter's signals based on the model. Another way to say this is that at an altitude of

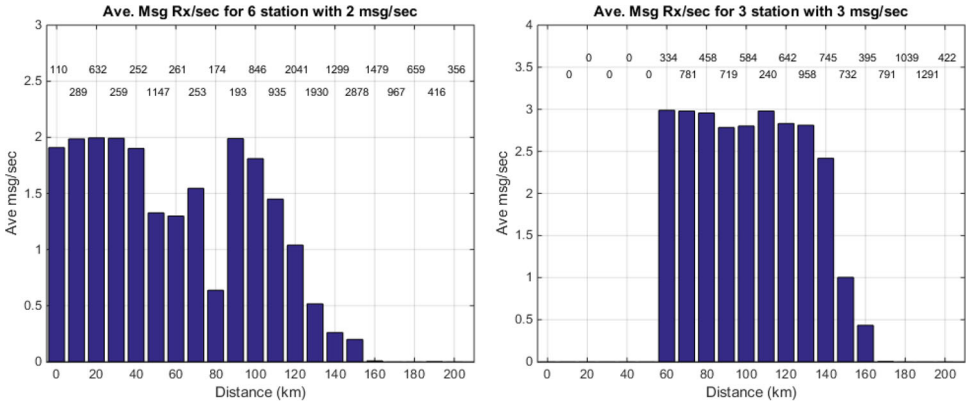

FIGURE 19 Average number of messages decoded per second versus distance for low- (left, 100% = 2 msg/sec) and medium- (right, 100% = 3 msg/sec) altitude tier stations (March 10, 2015, p.m.). Top number indicates seconds of data available for the average [Color figure can be viewed in the online issue, which is available at wileyonlinelibrary.com and www.ion.org]

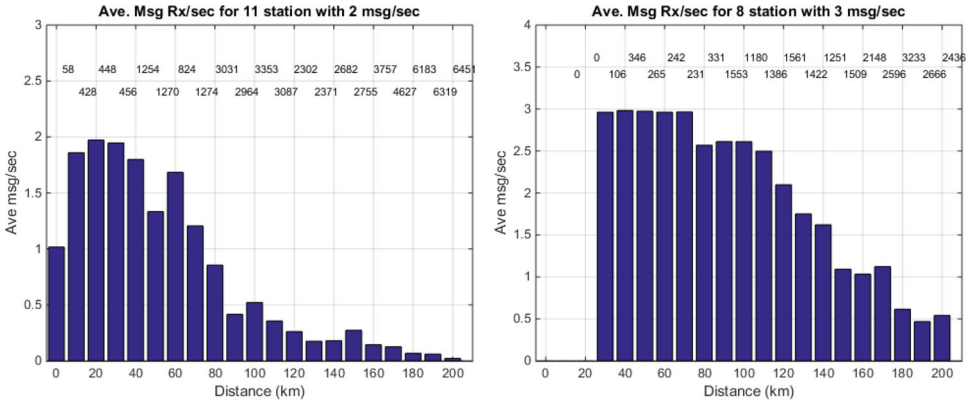

FIGURE 20 Average number of messages decoded per second versus distance for low- (left, 100% = 2 msg/sec) and medium- (right, 100% = 3 msg/sec) altitude tier stations (March 11, 2015, p.m.). Top number indicates seconds of data available for the average [Color figure can be viewed in the online issue, which is available at wileyonlinelibrary.com and www.ion.org]

1,145 m, the radio horizon of the transmitter at 25 m altitude (e.g. MSL) is 160 km at 1,145 m (in the same altitude frame). As reference, the radio horizon from the model at 4,000 ft MSL is 164.5 km. This seems to reasonably model our flight results shown in Figure 19 where complete loss of station reception occurs at a ground distance of around 160 km when flying at about 4,000 ft MSL. The radio horizon is where we would expect to start losing all messages from the station (goes to zero); we can see this happening on both plots of Figure 23 around 160 km where the message reception rates are well below expected, and at 170 km, there is essentially no message reception.

The modeling provides two important results. First, the 4/3 earth radius assumption is reasonable for estimating ADS-B UAT radio coverage. Second, there is a distinct reduction as well as return in message reception at distances well short of the radio horizon. This is strong evidence that there is strong intra-system interference. Since we experienced interference at around 80 km from the station, from the figure, we can see that the minimum visible at this distance is about 200 m (660 ft), which is quite low. Hence, even for approach and terminal airspace, intra-system interference may be an important consideration to tackle for UAT use as APNT.

$$d \approx \sqrt{2kRh_{tx}} + \sqrt{2kRh_{rx}} = \sqrt{2kR}\left(\sqrt{\mathrm{h_{tx}}} + \sqrt{\mathrm{h_{rx}}}\right) = 4.12\left(\sqrt{h_{tx}} + \sqrt{h_{rx}}\right)\ [km] \quad (12)$$

5.4 | Positioning

The flight altitudes and relatively flat terrain of Ohio mean that signals from multiple ADS-B radio stations can be received even at reasonably low altitudes out to roughly

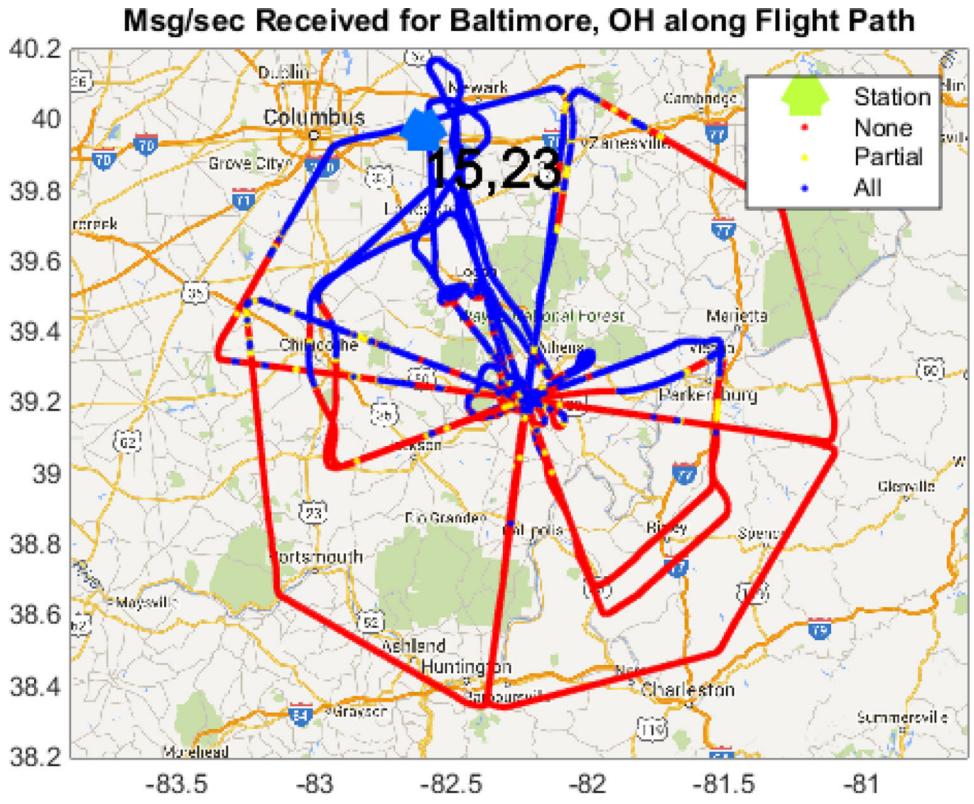

FIGURE 21 Reception map of Baltimore, OH, station (numbers indicate UAT ground segment slots assigned) [Color figure can be viewed in the online issue, which is available at wileyonlinelibrary.com and www.ion.org]

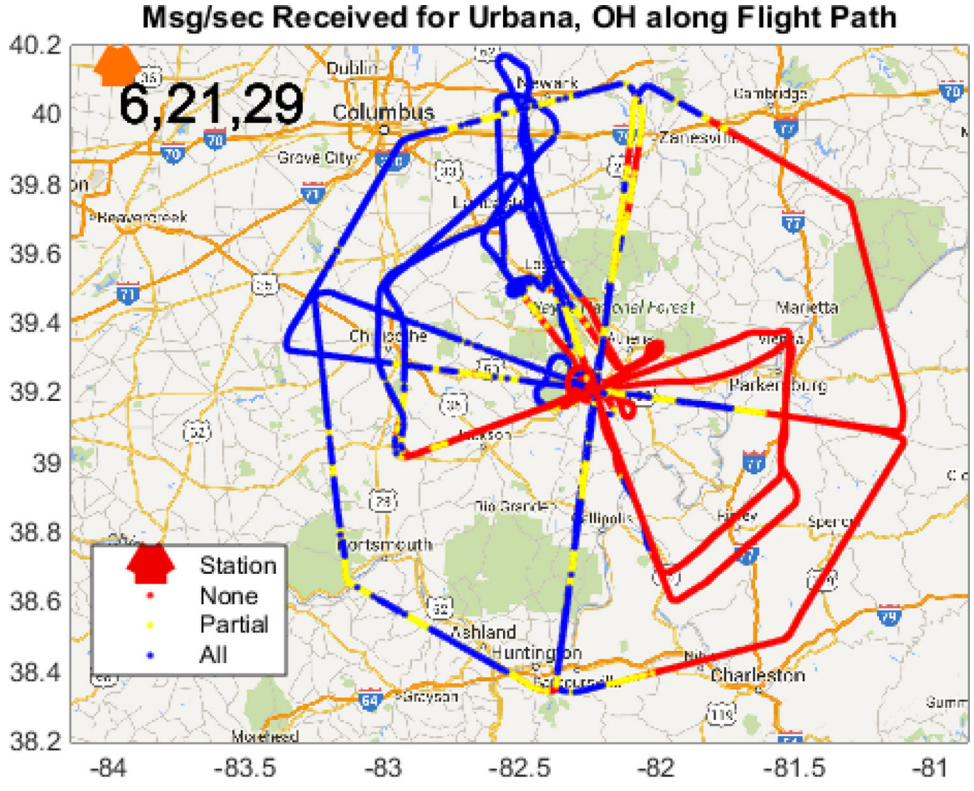

FIGURE 22 Reception map of Urbana, OH, station (numbers indicate UAT ground segment slots assigned) [Color figure can be viewed in the online issue, which is available at wileyonlinelibrary.com and www.ion.org]

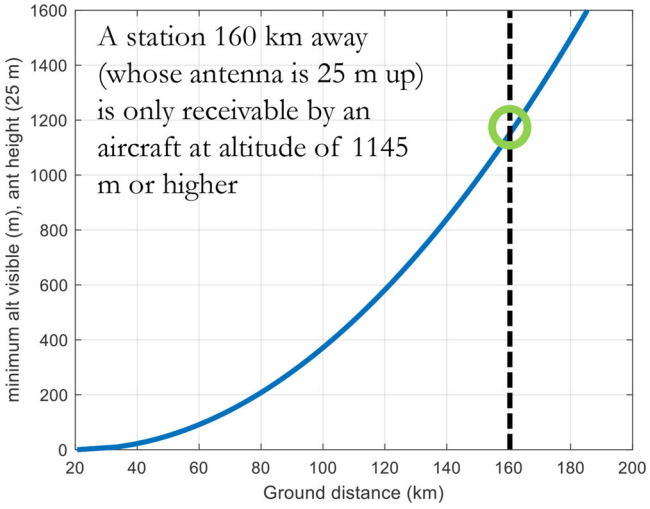

FIGURE 23 Minimum altitude at which an L-band signal is in radio line of sight from a 25 m tower versus distance from the tower (radio horizon model using 4/3 earth radius assumption) [Color figure can be viewed in the online issue, which is available at wileyonlinelibrary.com and www.ion.org]

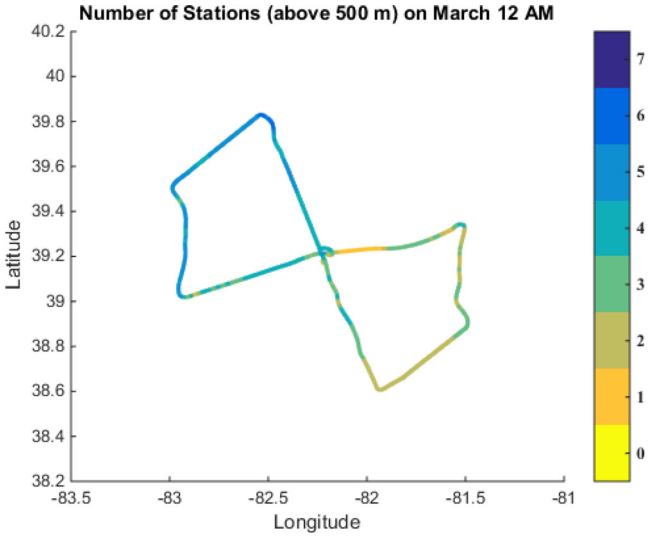

FIGURE 24 Number of stations per time epoch on March 12, 2015, a.m. flight (cruise at 3,300 ft MSL) [Color figure can be viewed in the online issue, which is available at wileyonlinelibrary.com and www.ion.org]

the ideal radio horizon based on modeling with a 4/3 earth radius. Given the stations available, this range is sufficient for positioning even at altitudes of 3,000 ft MSL or lower. Figure 24 and Figure 25 show the number of stations where we measure pseudorange for the flights on March 11 p.m. (~3,300 ft MSL) and March 13 (~10,500 ft MSL), respectively. Comparing the figures, the number of stations measured increases for the higher-altitude flight.

An initial assessment of positioning is based on two position solution techniques: 1) Bancroft's method and 2) an

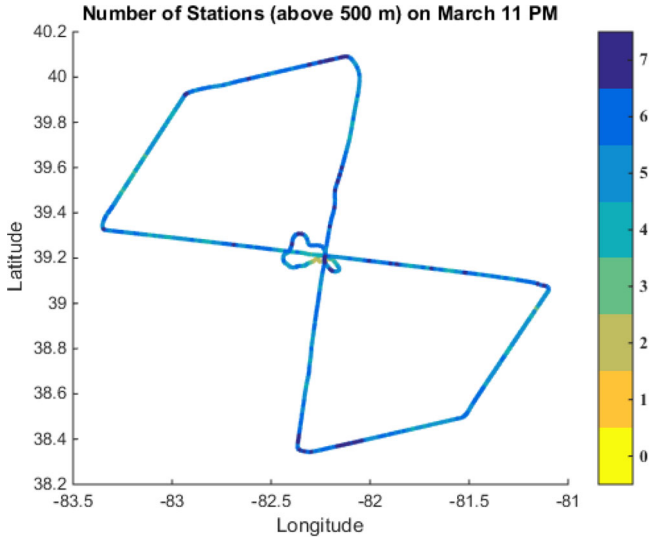

FIGURE 25 Number of stations per time epoch on March 11, 2015, p.m. flight (cruise at 10,500 ft MSL) [Color figure can be viewed in the online issue, which is available at wileyonlinelibrary.com and www.ion.org]

iterative solution (Nossek et al., 2014). Bancroft's method is a closed-form positioning solution, whereas the iterative solution requires an initial guess for position. The iterative solution is sensitive to the initial guess, and a poor guess can cause the method to not converge to a solution. In the analysis shown in this paper, we examined two methods: 1) a combination of the two methods where the closed-form Bancroft's solution is used to get an initial position estimate for an iterative solution (Jheng, et al., 2020; Nossek, et al., 2014), and 2) the iterative method with an initial guess used being the true location offset by about 7 kilometers horizontally.

For aircraft navigation, the signals only need to provide a horizontal position solution, as a barometric altimeter will provide the altitude information. For the analysis, GNSS altitude was used as a substitute altitude source. Bancroft's method and the iterative solution method were adapted to take an externally provided altitude and solve for the horizontal position and time with only three measurements. Our adapted Bancroft's method also required an estimate of the clock bias.

Figure 26 and Figure 27 show the positions from GPS, UAT with an initial estimate from March 12 a.m. (3,300 ft MSL) and March 11 p.m. (10,500 ft MSL). At 3,000 feet MSL, there are some parts of the flight where a position could not be calculated, as there were fewer than three signals. For flights at 10,000 feet, we generally had no problem with having an adequate number of signals for positioning. The increase in available signals from increasing altitude more than offsets the losses due to increased interference.

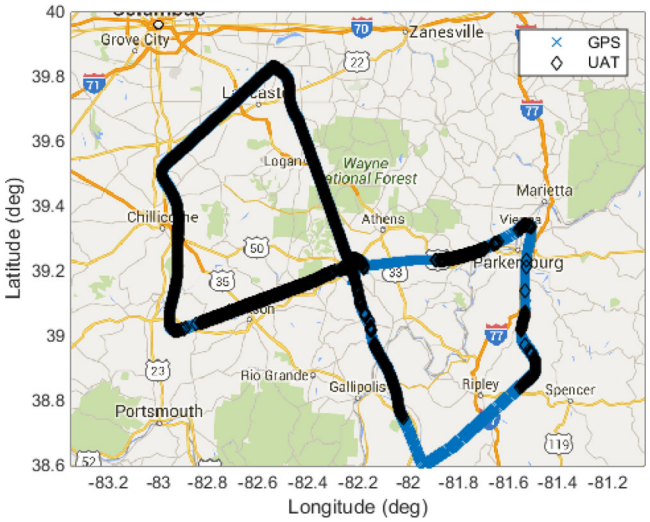

FIGURE 26 Position results using GPS, UAT (iterative based on close initial guess) March 12 a.m. flight (minimum altitude of 300 m above ground level (AGL)) [Color figure can be viewed in the online issue, which is available at wileyonlinelibrary.com and www.ion.org]

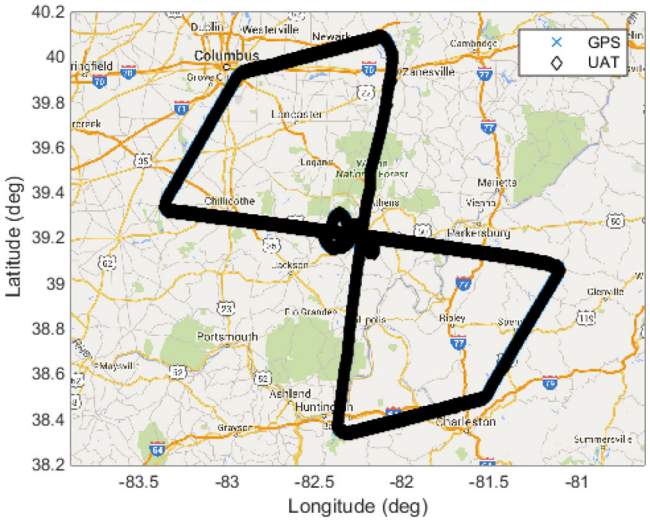

FIGURE 27 Position results using GPS, UAT (iterative based on close initial guess) March 11 p.m. flight (minimum altitude of 300 m above ground level (AGL)) [Color figure can be viewed in the online issue, which is available at wileyonlinelibrary.com and www.ion.org]

Figure 28 shows the distribution of the error in horizontal position for flights in the previous paragraph when solved using the iterative method with an initial guess offset from the true position by 70 km. Only converged solutions are shown. Furthermore, the solutions shown are also filtered to those having Dilution of Precision (DOP) less than 10 and being within 10 km of the actual point used. The former criterion rules out cases of poor geometry. The latter, as we shall see, eliminates solutions that converge to a different minimum or that are influenced by an outlier pseudorange. These requirements seem reasonable, as the navigator should have a previous solution that is within a short distance of the current position. The mean and standard deviation of error are around 30 m. The position errors are generally similar when using the combined methodology (i.e. Bancroft's method to provide initial estimate). Table 5 shows a comparison of results from the March 11 p.m. flight test using different initial estimates: 1) Bancroft's method, 2) initial estimate that is offset from the true position by 0.5 degrees in latitude and longitude (this is equivalent to a 70 km initial error), and 3) initial guess with a 0.05 degree offset in latitude and longitude (equivalent to 7 km initial error). The error for all calculated positions is large for the first two methods – this is due to convergence to the wrong solution. The third initial estimate method has much lower errors: mean and standard deviation of 29 m and 22 m. It also has all points used by the previous two methods suggesting that the errors in those methods are due to convergence. The table also separates the results to show the statistics for final positions with errors less and greater than 10 km. For final positions with errors <= 10 km, the error statistics for all methods are very similar and also represent a majority of points (~ 8,000). For final positions with errors > 10 km, the error statistics for the first two methods are in the tens of kilometers and represent about 1% of all points (55 and 87 out of over 8,000). Using Bancroft's method for initial estimate produced a few more instances with large errors as, in those instances, the Bancroft's method produced initial positions that were very far from the true position. There are no instances with large final position error when we have a better initial estimate (method three) even though that analysis contains every instance used in the previous two methods. This again indicates that the position calculated depends on initial guess, and a large outlier position solution is a convergence issue.

6 | CONCLUSIONS

This paper develops and demonstrates the use of UAT signals from FAA ADS-B radio stations for timing and ranging. It develops means of calculating pseudoranges from UAT transmissions, even those from the ADS-B segment. The technique is demonstrated on static ground tests with on-air signals. It then provides flight test results demonstrating actual performance in the air and measurements of intra-system interference. It shows for the first time some of the benefits and challenges of using UAT signals for navigation and timing. Specifically, we perform the first positioning using UAT signals that we

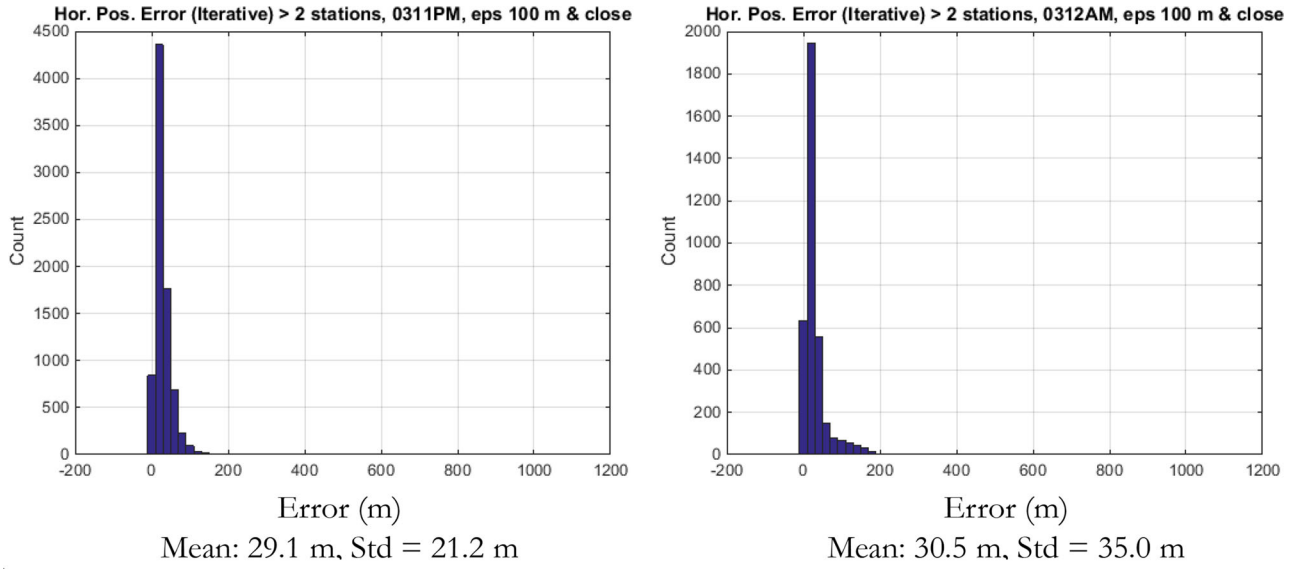

FIGURE 28 Histogram of position error from March 11 p.m. (left) and 12 a.m. (right) flight; limit DOP < 10 [Color figure can be viewed in the online issue, which is available at wileyonlinelibrary.com and www.ion.org]

TABLE 5 Comparison of positioning performance using iterative solution with different initial estimate sources: Bancroft's method and initial guesses in error from truth (simulates using prior positions): March 11 p.m. flight

	All calculated positions			Positions with errors < = 10 km			Positions with errors > 10 km		
Method for initial estimate	**Mean err (m)**	**Stan. Dev. err (m)**	**Number of Pts**	**Mean err (m)**	**Stan. Dev. err (m)**	**Number of Pts**	**Mean err (m)**	**Stan. Dev. err (m)**	**Number of Pts**
Bancroft	960	10,441	8,143	29.3	21.5	8,056	81,946	54,765	87
0.5°error (70 km) from true lat/lon	389	4,771	8,581	29.1	21.2	8,526	53,000	23,975	55
0.05°error (7 km) from true lat/lon	29.5	22.3	8,586	29.5	22.3	8,586	N/A	N/A	0

know of, and the results show an accuracy level suitable for navigation's most stringent APNT targeted operation such as Required Navigation Performance of 0.3 nautical miles (RNP 0.3). Better than 100 m position accuracy was achieved. UAT intra-system interference effects at altitude are measured. While these effects are not important for ADS-B or time synchronization and transfer, as one clear signal should always be available, they are a potential problem for navigation use. Analysis demonstrates the interference decreases coverage, especially for the low-altitude tier station. Fortunately, our flight tests showed the loss occurs at higher altitudes where we can receive plenty of other UAT stations. Also, the losses in the flight tests generally only occurred when interfered stations were 80 km or more away. There is less interference at low altitudes where improved coverage for APNT is most needed. For safety-of-life operations, the effect of the interference on range errors should be an integrity consideration when treating a signal for navigation and is worth exploring in future assessments.

ACKNOWLEDGEMENTS

The authors would like to thank the FAA Navigation Services Directorate for supporting this work. We also appreciate the help of Ohio University, in particular Wouter Pelgrum, Kuangmin Li, Adam Naab-Levy, and Jamie Edwards. We also acknowledge Shiwen Zhang and Nicolas Schneckenburger for their contributions. We would also like to acknowledge the late Professor Per Enge for his guidance and overall generosity.

DISCLAIMERS

The views expressed herein are those of the authors and are not to be construed as official or reflecting the views

of the Federal Aviation Administration or Department of Transportation.

ORCID

Sherman Lo https://orcid.org/0000-0002-4814-6506

REFERENCES

Chen, Y.-H., Lo, S., Jan, S.-S. J., Liu, G.-J., Akos, D., & Enge, P. (2014). Design and Test of Algorithms and Real-Time Receiver to use Universal Access Transceiver (UAT) for Alternative Positioning Navigation and Timing (APNT). *Proc. of the 27th International Technical Meeting of the Satellite Division of the Institute of Navigation (ION GNSS+ 2014)*, Tampa, FL.

Eldredge, L., Enge, P., Harrison, M., Kenagy, R., Lo, S., Loh, R., Lilly, R., Narins, M., & Niles, R. (2010). Alternative positioning, navigation & timing (PNT) study. *International Civil Aviation Organisation Navigation Systems Panel (NSP), Working Group Meetings*, Montreal, Canada. http://citeseerx.ist.psu.edu/viewdoc/download?doi=10.1.1.299.990&rep=rep1&type=pdf

Executive Office of the President. (2020). Executive Order 13905: Executive order on strengthening national resilience through responsible use of positioning, navigation, and timing (PNT) services. https://www.federalregister.gov/documents/2020/02/18/2020-03337/strengthening-national-resilience-through-responsible-use-of-positioning-navigation-and-timing

Federal Aviation Administration. (March 2004). Loran's capability to mitigate the impact of a GPS outage on GPS position, navigation, and time applications. *FAA report to FAA Vice President for Technical Operations Navigation Services Directorate*.

Federal Aviation Administration Surveillance and Broadcast Services (SBS) Program Office. (2013). *SBS Description Document SRT-047, Revision 02*.

Federal Aviation Administration. (2018). ADS-B ground stations as of 08-31-2018. https://www.faa.gov/foia/electronic_reading_room/media/ADS-B_Ground_Stations_as_of_08-31-2018.pdf

Haslett, C. (2008). *Essentials of radio wave propagation* (pp. 119–120). Cambridge University Press. https://doi.org/10.1017/CBO9780511536762

Jheng, S.-L., Jan, S.-S., Chen, Y.-H., Lo, S. (2020). 1090 MHz ADS-B-based wide area multilateration system for alternative positioning navigation and timing. *IEEE Sensors Journal*, *20*(16), 9490–9501. https://doi.org/10.1109/JSEN.2020.2988514

Kim, O.-J., & Kee, C. (2019). Single station–based precise positioning system: multiple-antenna arrangement for instantaneous ambiguity resolution. *NAVIGATION*, *66*(4), 747–768. https://doi.org/10.1002/navi.329

Li, K. & Pelgrum, W. (2014). A non-uniform DFT-based batch acquisition method for enhanced DME (eDME) carrier phase: Concept, simulations, and flight test results. *Proc. of the Institute of Navigation/Institute of Electronics and Electrical Engineers Position Location and Navigation Symposium (PLANS)*, Monterey, CA, 864–881. https://doi.org/10.1109/PLANS.2014.6851453

Lilley, R. W., & Erikson, R. (2012). DME/DME for alternate position, navigation, and timing (APNT). *FAA White Paper*. https://www.faa.gov/about/office_org/headquarters_offices/ato/service_units/techops/navservices/gnss/library/documents/apnt/media/20120723apnt_dmewhitepaper_dc.pdf

Lo, S. (2012). Pseudolite alternatives for alternate positioning, navigation, and timing (APNT), *FAA White Paper*. https://www.faa.gov/about/office_org/headquarters_offices/ato/service_units/techops/navservices/gnss/library/documents/apnt/media/APNT_Pseudolite_WhitePaper_Final.pdf

Lo, S., & Chen, Y.-H. (2020). Message design for a robust time signal using distance measuring equipment (DME) pulse pair position modulated (PPPM) pseudo lite. *European Navigation Conference*. https://doi.org/10.23919/ENC48637.2020.9317492

Lo, S., Chen, Y.-H., Enge, P., & Narins, M. (2015). Techniques to provide resilient alternative positioning, navigation, and timing (APNT) using Automatic Dependent Surveillance - Broadcast (ADS-B) ground stations. *Proc. of the 2015 International Technical Meeting of the Institute of Navigation*, Dana Point, CA.

Lo, S., Chen, Y.H., Enge, P., Pelgrum, W., Li, K., Weida, G., & Soelter, A. (2020). Flight test of a pseudo-ranging signal compatible with existing distance measuring equipment (DME) ground stations. *NAVIGATION*, *67*(3), 567–581. https://doi.org/10.1002/navi.376

Lo, S., Chen, Y.-H., & Enge, P. (2014). Hybrid APNT: Terrestrial Radionavigation to Support Future Aviation Needs. *Proc. of the 27th International Technical Meeting of the Satellite Division of the Institute of Navigation (ION GNSS+ 2014)*, Tampa, FL, 3029–3039.

Lo, S. C., Enge, P. K., & Narins, M. J. (2015). Design of a passive ranging system using existing distance measuring equipment (DME) signals & transmitters. *NAVIGATION*, *62*(2), 131–149. https://doi.org/10.1002/navi.83

Lo, S., Peterson, B., Akos, D., Narins, M., Loh, R., & Enge, P. (2011). Alternative position navigation & timing (APNT) based on existing DME and UAT ground signals. *Proc. of the 24th International Technical Meeting of the Satellite Division of the Institute of Navigation*, Portland, OR, 3309–3317.

Millman, G. H. (1958). Atmospheric effects on VHF and UHF propagation. *Proc. of the IRE*, *46*(8), 1492–1501. https://doi.org/10.1109/JRPROC.1958.286970

Niles, F. A., Conker, R. S., El-Arini, M. B., O'Laughlin, D. G., & Baraban, D. V. (2012). Wide area multilateration for alternate position, navigation, and timing (APNT). *FAA White Paper*. https://www.faa.gov/about/office_org/headquarters_offices/ato/service_units/techops/navservices/gnss/library/documents/APNT/media/WAM_WhitePaperFINAL_MITRE_v2.pdf

Nossek, E., Suess, M., Belabbas, B., & Meurer, M. (2014). Analysis of position and timing solutions for an APNT-System – A look on convergence, accuracy and integrity. *Proc. of the 27th International Technical Meeting of the Satellite Division of the Institute of Navigation*, Tampa, FL 3040-3047.

RTCA Special Committee-186 (2009). *Minimum operational performance standards for Universal Access Transceiver (UAT) Automatic Dependent Surveillance Broadcast (ADS-B)*. Washington, DC: RTCA.

Schneckenburger, N., Elwischger, B., Shutin, D., Suess, M., Belabbas, B., & Circiu, M-S. (2013). Positioning results for LDACS1 based navigation with measurement data. *Proc. of the 26th International Technical Meeting of the Satellite Division of the Institute of Navigation*. Nashville, TN, 772–781.

Schneckenburger, N., Fiebig, U.-C., Lo, S., Enge, P., & Lilley, R. (2018). Characterization and mitigation of multipath for

terrestrial based aviation radionavigation. *NAVIGATION*, *65*(2), 143–156. https://doi.org/10.1002/navi.235

White House Administrative Office. (2004). NSPD-39: U.S. space-based positioning, navigation, and timing policy. https://rosap.ntl.bts.gov/view/dot/16920

Wikipedia. Line-of-sight propagation. https://en.wikipedia.org/wiki/Line-of-sight_propagation

How to cite this article: Lo S, Chen Y-H. Automatic Dependent Surveillance-Broadcast (ADS-B) Universal Access Transceiver (UAT) transmissions for Alternative Positioning, Navigation, and Timing (APNT): Concept & practice. *NAVIGATION*. 2021;*68*(2):293–313. https://doi.org/10.1002/navi.424